Protein Binding

DOI: 10.1002/anie.201208688

Probing Target Search Pathways during Protein–Protein Association by Rational Mutations Based on Paramagnetic Relaxation Enhancement**

*Tae-Kyung Yu, Young-Joo Yun, Ko On Lee, and Jeong-Yong Suh**

Protein–protein association can be viewed as diffusion-controlled intermolecular collisions that form an ensemble of short-lived nonspecific encounter complexes, followed by the formation of a functional stereospecific complex. The existence of pre-equilibrium encounter complexes has long been predicted by Brownian dynamics simulations and kinetics experiments.[1] Recent application of NMR paramagnetic relaxation enhancement (PRE) spectroscopy combined with site-specific spin-labeling has offered new insights into the physicochemical nature of transient encounter complexes in protein–DNA[2] and protein–protein complexes.[3] Paramagnetic relaxation can reach up to approximately 34 Å for Mn^{2+} ions owing to the large gyromagnetic ratio of an unpaired electron. When lowly populated metastable species are in fast exchange with a stereospecific complex, measured intermolecular PREs are encoded by the distance information from the minor species (encounter complexes), in addition to the predominant species (stereospecific complex). Experimental PREs that do not agree with the calculated PREs from a stereospecific complex have been interpreted as a contribution from a nonspecific encounter-complex ensemble.

Transient encounter complexes have first been visualized between the N-terminal domain of Enzyme I (EIN) and the phosphocarrier HPr of the bacterial phosphotransferase system.[3a] Ensemble-simulated annealing refinement against experimental PREs has revealed that the distribution of nonspecific encounter complexes between EIN and HPr depends on the electrostatic surface potentials of the interacting proteins.[3a,4a] This pioneering work demonstrated the spatial distribution of the encounter-complex ensemble, yet it has not been clear how many and which kinds of the minor species detected by PRE are productive encounter complexes.[5] Encounter complexes can be productive if they make their way to a final stereospecific complex, or non-productive if they dissociate back to the free individual proteins (Figure 1). Herein, we employed rational mutations based on experimental PREs 1) to distinguish between productive and non-productive encounter complexes; and 2) to probe a possible target search pathway. Briefly, potential hot-spot residues for encounter complex formation detected by PRE are mutated, and equilibrium dissociation constants of the mutants are measured. If the mutation alters the equilibrium binding, intermolecular PREs are obtained to examine how the altered equilibrium binding relates with changes in the encounter complex formation.

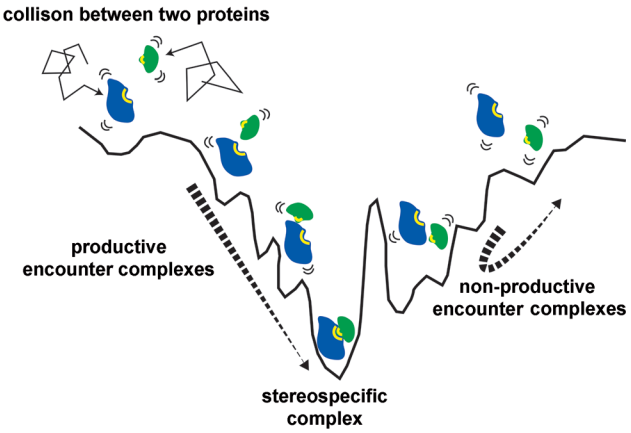

Figure 1. Illustration of protein–protein association on a reaction coordinate diagram. Two interacting proteins are shown in blue and green in a cartoon representation. Productive encounter complexes carry out a two-dimensional search until they fall into the free-energy minimum and form a stereospecific complex. Non-productive encounter complexes do not reach the stereospecific complex and dissociate back to the free proteins.

We designed mutants that could perturb the encounter complex formation between EIN and HPr. Previous studies showed that EIN largely employed its negatively charged surfaces to interact with the positively charged surfaces of HPr in the encounter-complex ensemble.[3a] We designed EIN mutants in which surface-exposed negatively charged aspartate or glutamate residues were replaced by positively charged lysine residues to perturb the electrostatic interaction. The EIN mutation sites were selected using the following criteria: 1) residues that exhibited PREs attributable to the encounter complexes, as identified in PRE profiles using spin-labeled HPr at positions 5 (E5C), 25 (E25C), or 32 (E32C);[3a,4a] and 2) residues that were located away from

[*] T. K. Yu, Y. J. Yun, K. O. Lee, Prof. J. Y. Suh
WCU Biomodulation Major, Department of Agricultural Biotechnology, Seoul National University
1 Gwanak-ro, Gwanak-gu, Seoul 151-921 (South Korea)
E-mail: jysuh@snu.ac.kr

[**] This work was supported by the World Class University program (R31-10056), and by a National Research Foundation of Korea (NRF) grant funded by the Ministry of Education, Science and Technology (2011-0025901 and 2010-0025883). We thank the high-field NMR facility at Korea Basic Science Institute for NMR experiments.

Supporting information for this article is available on the WWW under http://dx.doi.org/10.1002/anie.201208688.

the binding interface with HPr. Five EIN mutants were designed as follows: EINmut1 was designed based on the PRE profile of the EIN-E25C complex; EINmut2 and EINmut3 were designed based on the PRE profile of the EIN-E5C complex; EINmut4 and EINmut5 were designed based on the PRE profile of the EIN-E32C complex (Supporting Information, Figure S1 and Table S1). EINmut1 included mutations in the loop between the α1 and α2 helices, and the other four EIN mutants included mutations in helices α1, α2, α2′, and α3. The positions of the mutation sites in each EIN mutant are shown in the three-dimensional structure of the EIN-HPr complex in Figure 2.

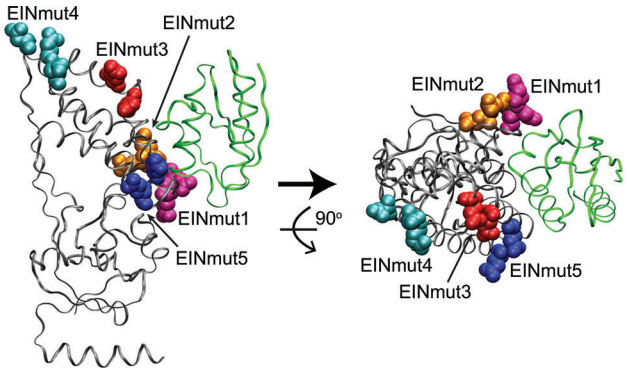

Figure 2. Three-dimensional structure of the specific EIN(gray)-HPr-(green) complex (PDB ID: 3EZA), shown as a ribbon diagram. The mutation sites introduced to EIN are shown with space-filling models: EINmut1 = magenta, EINmut2 = orange, EINmut3 = red, EINmut4 = cyan, and EINmut5 = blue. The mutated residues of the individual EIN mutants are described in detail in Table S1 (Supporting Information). Left panel: front view; right panel: top view.

We obtained the circular dichroism (CD) spectra of EIN and the EIN mutants to examine whether the introduced mutations perturbed the secondary structures of EIN. The CD spectra showed that the secondary structures in the EINmut1 were significantly disrupted by the mutation, whereas the other four mutants maintained a secondary-structure profile similar to that of EIN (Supporting Information, Figure S2). In the EINmut1, mutations at Asp119 and Glu121 most likely disrupted the salt bridges between the carboxylic acid side chains and the neighboring Lys124, which could be deleterious to the proper folding of the protein. Therefore, we excluded EINmut1 from further analysis.

We examined the equilibrium binding between EIN (or EIN mutants) and HPr using isothermal titration calorimetry (ITC). The equilibrium dissociation constant (K_D) between EIN and HPr was measured to be 4.8 μM, consistent with previous reports.[4a] EIN mutants generally showed a reduced binding affinity for HPr, but the magnitude of the reduction varied between the mutants (Table 1 and Supporting Information, Figure S3). EINmut2 and EINmut4 showed a twofold decrease of K_D (approximately 8–10 μM) for HPr, while EINmut5 exhibited a comparable binding affinity for HPr to that of EIN (Table 1). EINmut3 showed the largest reduction in the binding affinity for HPr, with a K_D of 51 μM, a factor of ten higher than that of the EIN-HPr complex. We further

Table 1: Thermodynamic parameters for the interaction between EIN (or EIN mutants) and HPr.

	K_D[a] [μM]	ΔG[b] [kcal mol^{-1}]	ΔH[c] [kcal mol^{-1}]	ΔS[d] [cal mol^{-1} deg^{-1}]
EIN	4.8 ± 0.7	−7.6 ± 0.09	3.7 ± 0.1	36.3 ± 0.4
EINmut2	9.9 ± 0.9	−7.1 ± 0.06	3.5 ± 0.1	34.3 ± 0.4
EINmut3	51.0 ± 0.7	−6.1 ± 0.08	5.7 ± 0.4	37.9 ± 1.3
EINmut3a	13.9 ± 1.8	−6.9 ± 0.08	4.1 ± 0.2	36.3 ± 0.7
EINmut3b	16.5 ± 2.0	−6.8 ± 0.07	4.3 ± 0.1	37.8 ± 0.4
EINmut4	8.4 ± 1.0	−7.2 ± 0.07	4.2 ± 0.1	36.9 ± 0.4
EINmut5	5.2 ± 0.4	−7.6 ± 0.05	4.2 ± 0.1	37.8 ± 0.4

[a] Equilibrium dissociation constant; [b] binding free energy; [c] binding enthalpy; [d] binding entropy.

investigated EINmut3 variants where the negatively charged residues were replaced by neutral residues instead of the positively charged lysines. When Glu81 and Glu86 were replaced by isosteric glutamine (EINmut3a) or alanine residues (EINmut3b), the K_D values were 14 μM and 17 μM, respectively; hence the neutral mutations made an intermediate reduction of the equilibrium binding compared to the charge-reversed mutation. Note that the EIN mutants examined in this study were designed in view of the PREs associated with the encounter-complex ensemble. Also, the mutation sites were selected such that they would not interfere with the binding interface in the stereospecific complex. The fact that the EIN mutants displayed a varying degree of reduction in their equilibrium binding with HPr suggests that the encounter complexes detected by PRE contribute to the specific complex formation to differing degrees, depending on their locations. Mutations that perturb the formation of productive encounter complexes likely have a larger impact on the equilibrium binding than those that perturb the formation of non-productive encounter complexes. To investigate how these mutations affected the formation of the encounter complex, we measured the intermolecular PREs of EIN, EINmut3, EINmut3a, and EINmut2 in complex with E5C.

The NMR samples used for the PRE measurement comprised 0.3 mM $^{2}H/^{15}N$-labeled EIN (or EIN mutants) and 0.5 mM HPr in 20 mM Tris-HCl, pH 7.4. HPr was spin-labeled by conjugating EDTA-Mn^{2+} to HPr by way of disulfide linkage to the surface-engineered cysteine residue at position 5 (E5C). We performed the three-dimensional triple-resonance through-bond scalar correlation HNCACB and CBCA(CO)NH experiments using $^{2}H/^{13}C/^{15}N$-labeled EIN mutants for the backbone assignment (Supporting Information, Figure S4 for EINmut3). In particular, the lysine residues were carefully assigned by 2D ^{1}H-^{15}N heteronuclear single quantum correlation (HSQC) spectra of [^{15}N-Lys]-EIN mutants, which were prepared using amino acid-selective labeling with ^{15}N-lysine as a precursor. The intermolecular backbone $^{1}H_N$ PRE rates (Γ_2) were obtained by measuring the differences between the R_2 relaxation rates of the paramagnetic and diamagnetic samples at 37 °C using a TROSY-based pulse scheme at a ^{1}H frequency of 800 MHz.[6] Experimental PREs of EIN, EINmut3, and EINmut3a are shown as red circles, and calculated PREs

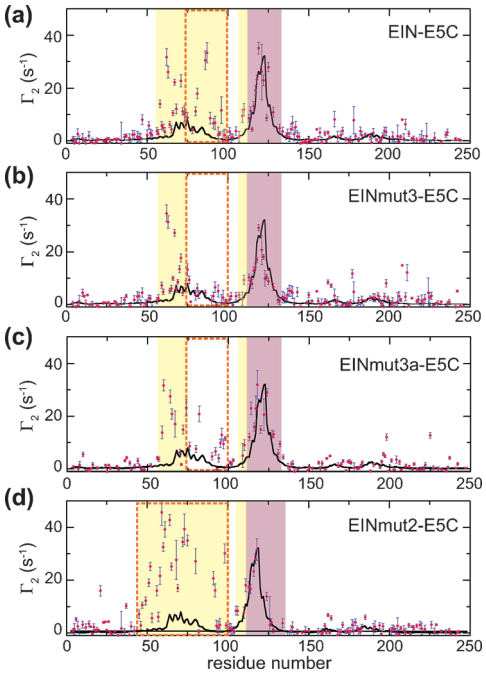

Figure 3. Comparison of the observed and calculated intermolecular PREs for the a) EIN-E5C, b) EINmut3-E5C, c) EINmut3a-E5C, and d) EINmut2-E5C complexes. The observed intermolecular $^{1}H_{N}$-Γ_2 rates (red circles) and back-calculated values (black line) are shown with error bars. PREs arising from the specific complex structure are highlighted in the purple boxes, and PREs attributable to the nonspecific encounter-complex ensemble are highlighted in the yellow boxes. Differences between the PRE profiles of the EIN and EIN mutants are shown in the dashed orange boxes.

from the EIN-E5C complex structure are shown as black lines in Figure 3a–c. Large PREs between residues 115 and 127 were predicted from the stereospecific complex structure, and PREs outside of this region were attributed to nonspecific encounter complexes. All three complexes showed PREs originating from the specific complex, consistent with the calculated values. By contrast, PREs attributed to the nonspecific encounter-complex ensemble clearly differed between the complexes. Large PREs appeared between residues 62 and 89 in the EIN-E5C complex, whereas large PREs showed up only between residues 62 and 75 in the EINmut3-E5C complex. Notably, the PREs attributable to the encounter-complex ensemble largely disappeared near the mutation sites in EINmut3 (residues 81 and 86), as highlighted by orange dashed boxes in the PRE profiles (Figure 3a,b). EINmut3a exhibited PREs attributable to the encounter complexes smaller than EIN but larger than EINmut3 near the mutation site (Figure 3c). We note that the intermediate magnitude of the PREs of EINmut3a correlates with its moderate reduction in binding affinity for HPr compared to EINmut3. This correlation suggests that encounter complex formation near the mutation site is mainly driven by electrostatic interactions, and is also directly linked to the specific complex formation. The three-dimensional structure of the EIN-HPr complex color-coded by PRE profiles clearly demonstrates that the encounter complexes mostly disappeared at the mutation site (Supporting Information, Figure S5).

We also measured PREs from the EINmut2-E5C complex, and the PREs predicted from the specific complex structure appeared similar between the EINmut2-E5C and EIN-E5C complexes (Figure 3d). On the other hand, PREs attributable to the nonspecific encounter-complex ensemble appeared in a wider region (residues 47–89) compared to EIN (residues 62–89), and also the magnitude of PREs in this region was slightly larger in EINmut2. The PREs from the EINmut2-E5C complex were reproducible from separately prepared samples. This indicates that the mutation in EINmut2 apparently affected the encounter complex formation in a region remote from the mutation site. Because the equilibrium binding of EINmut2-HPr was twice as weak as that of EIN-HPr, we suppose that the emerging encounter complexes in EINmut2 did not promote the equilibrium binding. In fact, PREs in EINmut2 mainly increased on helix α1, the mutation of which showed little change in the equilibrium binding, as shown in the EINmut5-HPr complex (Table 1). It is notable that surface-charge mutations can influence the encounter complex formation directly at the mutation site (e.g. EINmut3), or indirectly at a remote site (e.g. EINmut2).

We further investigated whether the reduced equilibrium binding of EIN mutants resulted from changes in the association (k_{on}) or dissociation (k_{off}) rate constants by qualitative line-shape analysis of ^{1}H-^{15}N correlation spectra during titration. When we titrated ^{15}N-HPr with EIN, the side-chain amide resonance of Gln51 showed a continual shift with line broadening, which was maximal when the fractional population of the complex was approximately 0.3 (Figure 4a). This indicates an exchange rate (k_{ex}) on the fast side of intermediate exchange, suggesting that $k_{ex} \approx 7500\ s^{-1}$ ($2\Delta\omega_{HN} < k_{ex} < 3\Delta\omega_{HN}$).[7] For a second-order exchange, $k_{ex} = k_{off} + k_{on}[EIN] = k_{off} + k_{off}[EIN\text{-}HPr]/[HPr] = k_{off}(1+P_{EIN\text{-}HPr}/P_{HPr})$, where [EIN], [HPr], and [EIN-HPr] are the concentrations of free EIN, free HPr, and EIN-HPr complex at equilibrium, respectively, and $P_{EIN\text{-}HPr}$ and P_{HPr} are the fractional population of EIN-HPr complex, and free HPr, respectively.[8] From this equation, k_{off} is estimated as $4400\ s^{-1}$, and k_{on} is approximately $9.2 \times 10^{8}\ M^{-1}s^{-1}$, which is of the same order of magnitude as the phosphoryl transfer reaction rate constant between Enzyme I and HPr from kinetic measurements.[9] Because HPr exhibited a similar line-broadening profile during the titration with EIN, EINmut3, and EINmut2, the dissociation rate constants would be comparable between these protein complexes (Figure 4a–c). Hence, the lower degree of binding (higher K_D) of the EIN mutants most likely resulted from the decrease of the association rate constants.

We examined chemical-shift perturbations, R_2 relaxation parameters, and residual dipolar couplings (RDCs) of amide groups for EINmut3, EINmut3a, and EINmut2 to confirm that these mutations did not alter the structure and dynamics of the protein. The chemical-shift perturbations were mostly localized to the mutation site and its vicinity (Supporting Information, Figure S6). Also, the ratio of the R_2 relaxation parameters of amide protons between individual mutants and

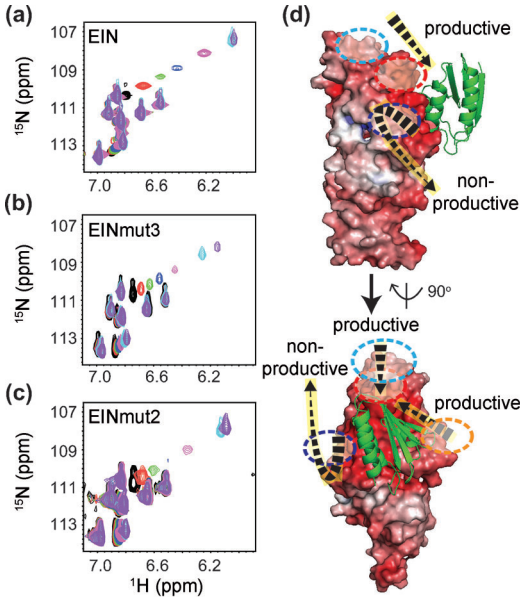

Figure 4. 2D ^{1}H-^{15}N HSQC spectra of ^{15}N-HPr titrated with a) EIN, b) EINmut3, and c) EINmut2. HPr (0.5 mM) was titrated with stoichiometric ratios of EIN(mut) protein of 0 (black), 0.1 (red), 0.2 (green), 0.3 (blue), 0.5 (magenta), 1 (cyan), and 2 (violet). The progressive chemical-shift perturbation of Gln51 is characteristic of the fast side of intermediate exchange. d) A model of target search pathways of the productive and non-productive encounter complexes between EIN and HPr. EIN is shown as a molecular surface representation color-coded by electrostatic potential ±12 kT, and HPr is shown as a ribbon diagram in green and forms a stereospecific complex with EIN. The mutation sites are denoted by dashed circles: EINmut2 = orange, EINmut3 = red, EINmut4 = cyan, and EINmut5 = blue.

EIN were uniform and close to unity, indicating that the dynamics of the protein are minimally perturbed by the mutations (Supporting Information, Figure S7). We finally measured the RDCs of the backbone amide to determine whether the mutations affected the folding of the backbone in the mutants. Measured $^{1}D_{NH}$ values showed excellent agreement with those calculated from the EIN-HPr coordinates (PDB ID: 3EZA; Supporting Information, Figure S8). Taken together, EINmut3, EINmut3a, and EINmut2 did not show significant changes in their structure and dynamics in the whole protein and also within the specific binding interface.

The data presented in this study suggest that the encounter complexes probed by the intermolecular PRE measurements play distinct roles in protein–protein association. Based on our current results, we propose a model of possible target search pathways during the association between EIN and HPr. The mutation sites of EINmut3 and EINmut4 are located above the specific binding interface, and those of EINmut2 and EINmut5 are at either side of the specific binding interface. The target search pathways in our model are as follows: HPr forms an encounter complex with EIN at a region above the specific binding interface and slides down toward the specific binding site. In addition, HPr can form an encounter complex with EIN at the side of the specific binding interface, but lateral sliding toward the specific binding interface is less efficient. In particular, sliding from the mutation site of EINmut5 is mostly restricted possibly owing to steric hindrance or less favorable electrostatic interactions guiding the encounters to the specific binding site. Figure 4 d summarizes the target search pathways by way of productive encounter complexes, and also unsuccessful attempts of non-productive encounter complexes. Note that the electrostatic surface potential of EIN alone does not discriminate between the interfaces for productive and non-productive encounter complexes. We infer that initial encounters are driven by long-range electrostatic attractions, but a successful journey from the encounter to the specific binding site requires favorable short-range interactions along the pathway as well.

The distinct nature of the encounter complexes has been predicted using Brownian dynamics simulations and kinetic measurements of several protein–protein complexes.[10] Because PRE was first used to visualize the encounter-complex ensemble, efforts have been made to characterize the physicochemical nature of the encounter complexes and also to understand the roles of the different encounter complexes in a specific complex formation.[4] We showed herein that the differential contributions of encounter complexes toward the specific complex formation can now be quantitatively evaluated by rationally designed mutants, and changes in the encounter complex formation of the mutants can be visually monitored. Further, experimental PREs combined with the thermodynamic parameters of equilibrium binding determine how much a particular hot-spot region for encounter complex formation contributes to the specific binding. For example, diminished encounter complexes of EINmut3 (charge reversal) and EINmut3a (charge neutralization) accounted for the free energy differences of binding, as much as approximately 1.5 kcal mol^{-1} and 0.7 kcal mol^{-1}, respectively, compared to EIN. The biological and evolutionary roles of non-productive encounter complexes are yet uncertain. When a protein interacts with multiple partner proteins, the hot-spot regions that form productive or non-productive encounter complexes can vary and sometimes may even switch their roles to discriminate different partner proteins. The exploration of target search pathways could eventually be applied to the manipulation of equilibrium binding in protein–protein or protein–ligand complexes without affecting their binding interface.

Received: October 30, 2012
Revised: December 27, 2012
Published online: February 12, 2013

Keywords: encounter complexes · equilibrium binding · NMR spectroscopy · paramagnetic relaxation enhancements · protein-protein interactions

[1] a) O. G. Berg, P. H. von Hippel, *Annu. Rev. Biophys. Biophys. Chem.* **1985**, *14*, 131–160; b) M. Vijayakumar, K. Y. Wong, G. Schreiber, A. R. Fersht, A. Szabo, H. X. Zhou, *J. Mol. Biol.* **1998**, *278*, 1015–1024; c) G. Schreiber, A. R. Fersht, *Nat. Struct. Biol.* **1996**, *3*, 427–431; d) J. Buck, B. Furtig, J. Noeske, J. Wohnert, H. Schwalbe, *Proc. Natl. Acad. Sci. USA* **2007**, *104*, 15699–15704.

[2] a) J. Iwahara, G. M. Clore, *Nature* **2006**, *440*, 1227 – 1230; b) G. M. Clore, C. Tang, J. Iwahara, *Curr. Opin. Struct. Biol.* **2007**, *17*, 603 – 616.
[3] a) C. Tang, J. Iwahara, G. M. Clore, *Nature* **2006**, *444*, 383 – 386; b) A. N. Volkov, J. A. R. Worrall, E. Holtzmann, M. Ubbink, *Proc. Natl. Acad. Sci. USA* **2006**, *103*, 18945 – 18950; c) C. Tang, J. Louis, A. Aniana, J. Y. Suh, G. M. Clore, *Nature* **2008**, *455*, 693 – 696; d) G. M. Clore, J. Iwahara, *Chem. Rev.* **2009**, *109*, 4108 – 4139; e) Q. Bashir, A. N. Volkov, G. M. Ullmann, M. Ubbink, *J. Am. Chem. Soc.* **2010**, *132*, 241 – 247; f) V. A. Villareal, T. Spirig, S. A. Robson, M. Liu, B. Lei, R. T. Clubb, *J. Am. Chem. Soc.* **2011**, *133*, 14176 – 14179.
[4] a) J. Y. Suh, C. Tang, G. M. Clore, *J. Am. Chem. Soc.* **2007**, *129*, 12954 – 12955; b) N. L. Fawzi, M. Doucleff, J. Y. Suh, G. M. Clore, *Proc. Natl. Acad. Sci. USA* **2010**, *107*, 1379 – 1384.
[5] T. L. Blundell, J. Fernandez-Recio, *Nature* **2006**, *444*, 279 – 280.
[6] J. Iwahara, C. Tang, G. M. Clore, *J. Magn. Reson.* **2007**, *184*, 185 – 195.
[7] J. Y. Suh, J. Iwahara, G. M. Clore, *Proc. Natl. Acad. Sci. USA* **2007**, *104*, 3153 – 3158.
[8] L. Y. Lian, G. C. K. Roberts in *NMR of Macromolecules* (Ed.: G. C. K. Roberts), Oxford University Press, Oxford, **1993**, pp. 153 – 182.
[9] N. D. Meadow, R. L. Mattoo, R. S. Savtchenko, S. Roseman, *Biochemistry* **2005**, *44*, 12790 – 12796.
[10] M. Harel, A. Spaar, G. Schreiber, *Biophys. J.* **2009**, *96*, 4237 – 4248.

